Supporting Information for

Unanticipated Stickiness of α-Pinene

Hilary M. Chase, Junming Ho, Mary Alice Upshur, Regan J. Thomson, Victor S. Batista, Franz M. Geiger*

S1. Molecular Orientation Comparison as a Function of α-Pinene Pressure and Temperatures.

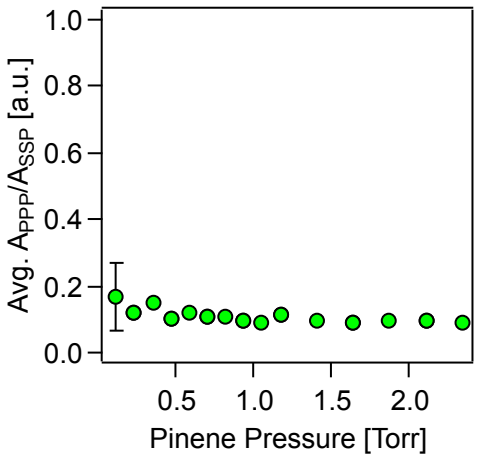

Figure S1. A_{PPP}/A_{SSP} ratios as a function of α-pinene pressure. Error bars indicate standard deviations of averaging trials.

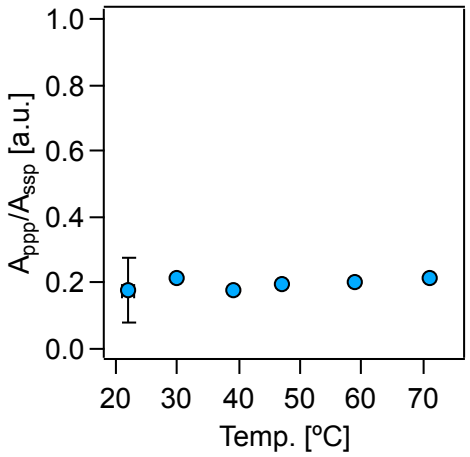

Figure S2. A_{PPP}/A_{SSP} ratios as a function of temperature. Error bars indicate standard deviations of averaging trials.

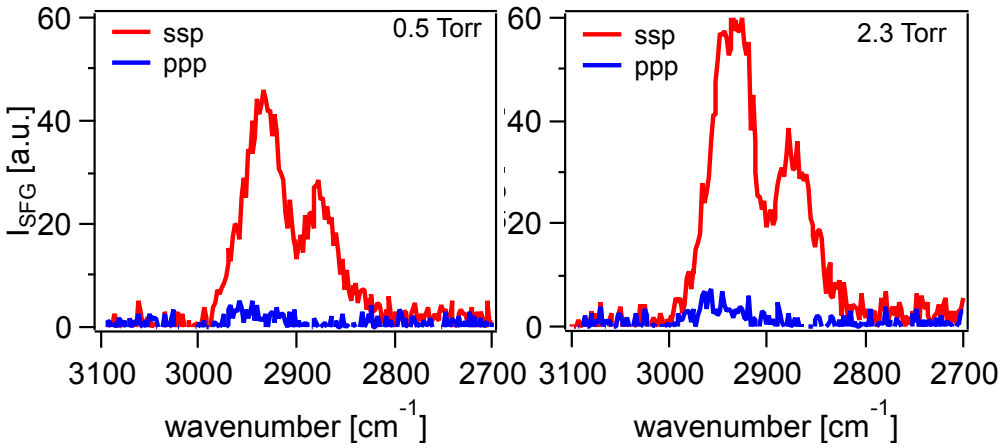

Figure S3. *Ssp* (red traces) and *ppp* (blue traces) spectra of α-pinene at two different vapor pressures, 0.47 Torr and 2.34 Torr.

S2. Pinene Vapor Pressure Calibration by Infrared Spectroscopy.

The Bruker Tensor 37 FTIR Spectrometer was used for this study in transmission mode, using approximately 32 scans at a 2 cm^{-1} spectral resolution. The spectrometer is outfitted with a Mid-IR detector and a KBr beamsplitter, and scanned between 400 and 4000 cm^{-1}.

The α-pinene vapor pressures reported were determined by taking the ratio of pinene flow rates to the total flow rate multiplied by the vapor pressure of neat α-pinene (3 Torr). We utilized FTIR spectroscopy to calibrate these pressures by injecting liquid pinene into the bottom of a 10 cm^{-1} pathlength vapor IR cell with a Pyrex body and NaCl windows (Model G-2 Gas Cell, International Crystal Laboratories), and closing the cell valves to ensure vapor equilibration. A maximum IR equilibrium vapor absorbance of 0.8 was correlated to a vapor pressure of 3 Torr at 20°C (Sigma-Aldrich), and was used to calibrate the remaining pinene pressures used in the experiments.

For the adsorption isotherm experiments, the various helium/pinene mixing ratios were initially purged through the gas cell for approximately 3 minutes. After purging, one cell valve was

closed and the cell was filled with the helium/pinene mixture for 1 minute. After spectral acquisition the cell was purged with dry nitrogen. The on-off trace experiments were carried out in 4 continuous 25-minute cycles, and IR spectra were taken every 5 minutes. An additional tube was attached to the second valve in the gas IR cell in order to vent the cell during the flow experiment.

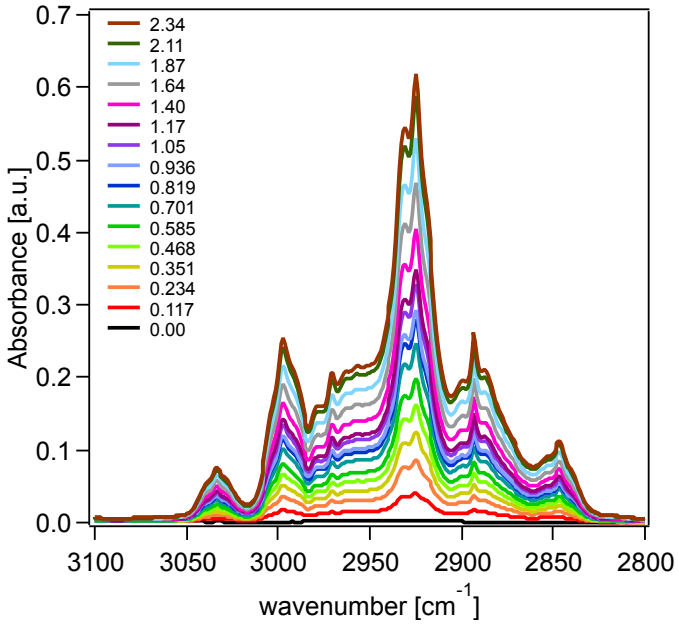

Figure S4. Representative trial of α-pinene pressure calibration by FTIR.

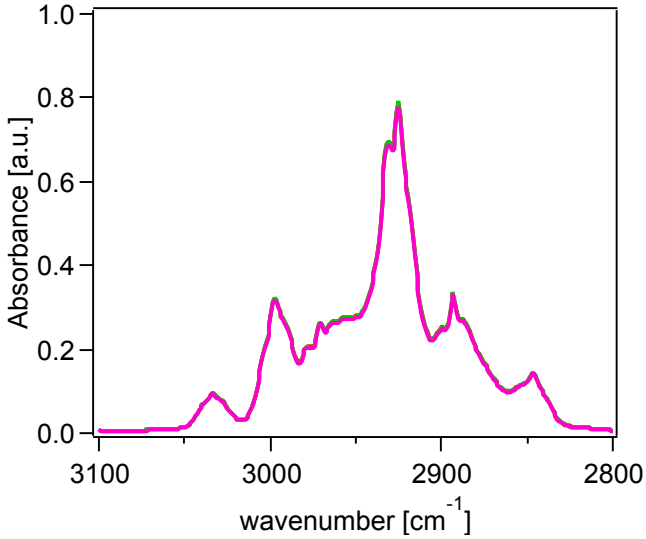

Figure S5. FTIR spectrum of vapor from liquid α-pinene in vapor cell.

S3. Experimental Controls. Controls were carried out to ensure that the residual α-pinene signal observed by SFG was not due to α-pinene left in the Teflon flow cell or O-ring. After α-pinene exposure, we replaced the α-pinene-exposed optical window with a clean optical window, and without cleaning the Teflon cell or o-ring no SFG signal was detected. Additionally, in order to confirm whether residual α-pinene within the flow setup tubing was contributing to the α-pinene SFG signal upon pure 5 SLPM helium exposure, we carried out this analogous experiment with FTIR. Upon switching from α-pinene to helium flow, the absorbance signal disappeared within less than one minute. These results are consistent for multiple cycles, indicating that α-pinene left in the tubing is not responsible for the residual signal observed by SFG.

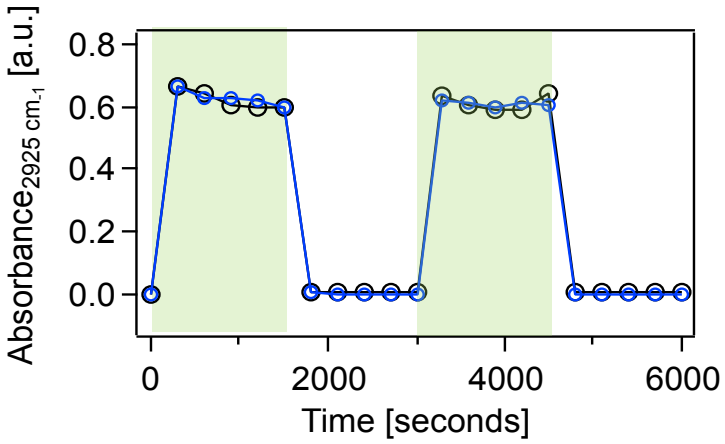

Figure S6. On-off trace of α-pinene vapor (green regions) and helium (white region). The maximum absorbance at 2925 cm^{-1} via FTIR is plotted over time in order to show that there is no residual α-pinene signal from tubing when pure helium flow is on.

S4. Hexane On-Off Trace.

We collected three on-off traces of hexane vapor on fused silica using the analogous experimental setup described in the main text. We find that hexane adsorption to fused silica is fully reversible.

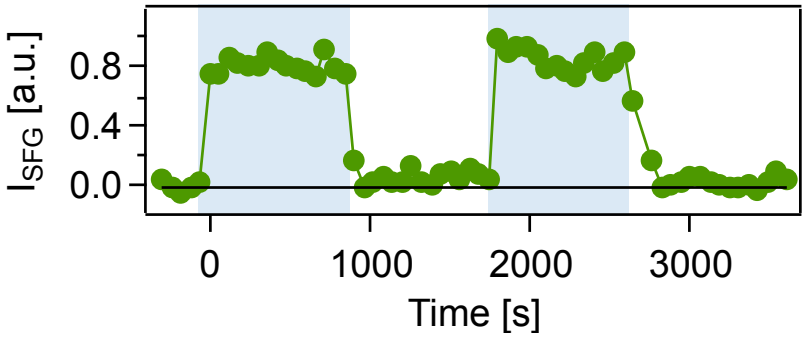

Figure S7. Average on-off trace of hexane vapor on fused silica plotting the maximum *ssp* SFG signal intensity (I_{SFG}) over time. The blue regions indicate where the hexane-saturated helium flow was on, and the white regions indicate where pure helium was on. The trace is an average of three individual trials, and has been normalized to the maximum SFG signal intensity.

S5. Adsorption Isotherm Fits.

A number of adsorption models were explored to determine which would be sufficient for modeling α-pinene adsorption to SiO_2. We explored the single-site Langmuir isotherm, dual-site Langmuir, Langmuir-Freundlich, dual-site Langmuir Freundlich, and dual site with reversibility. The subsequent van't Hoff plots are given below along with error bars associated with largest uncertainties in the K_{ads} from the fits. The fit equations are given below in Table S1.

When obtaining K_{Ads} from the various fit models, it is important to keep in mind units, because ultimately a unitless K_{Ads} is required for carrying out a proper van't Hoff analysis. In order to obtain a unitless $K°$ for our van't Hoff analysis, we corrected for the standard state while keeping the units in mind. Therefore, the following correction was made:

$$K^{\circ} = K\left(\frac{P^{\circ}\theta_S^{\circ}}{\theta_A^{\circ}}\right) \quad \text{(S1).}$$

where P° is 760 torr, and $\theta_S^{\circ} = \theta_A^{\circ} = 0.5$. θ_S° refer to the standard states for unoccupied surface sites, θ_A° represents the standard state for the adsorbate.

Table S1. Adsorption model equations used to fit temperature-dependent isotherms.

Model	Equation	Coefficients
Langmuir	$f(P) = \frac{a * KP}{1 + KP}$	a = monolayer coverage scaling factor K = adsorption constant (torr^{-1}) P = pinene pressure (torr)
Dual-Site Langmuir	$f(P) = \frac{a * K_1P}{1 + K_1P} + \frac{b * K_2P}{1 + K_2P}$	a = site 1 saturation capacity b = site 2 saturation capacity K_1 =site 1 adsorption constant (torr^{-1}) K_2 = site 2 adsorption constant (torr^{-1}) P = pinene pressure (torr)
Langmuir-Freundlich	$f(P) = \frac{a * (KP)^n}{1 + (KP)^n}$	a = monolayer coverage scaling factor n = heterogeneous parameter K =equilibrium constant (torr^{-1})^n P = pinene pressure (torr)
Dual-site Langmuir Freundlich	$f(P) = \frac{a * (K_1P)^n}{1 + (K_1P)^n} + \frac{b * (K_2P)^m}{1 + (K_2P)^m}$	a =site 1 saturation capacity K_1 =site 1 adsorption constant (torr^{-1})^n n =site 1 heterogeneous parameter b =site 2 saturation capacity K_2 =site 2 adsorption constant (torr^{-1})^n m =site 2 heterogeneous parameter P = pinene pressure (torr)
Dual site with irreversibility	$f(P) = Q + \frac{a * KP}{1 + KP}$	Q = irreversible constant a = monolayer coverage scaling factor K = adsorption constant (torr^{-1}) P = pinene pressure (torr)
Redlich-Peterson	$f(P) = \frac{AP}{1 + BP^g}$	A = R-P constant (torr^{-1}) P =pinene pressure (torr) B =adsorption constant (torr^{-1})^g g = heterogeneity term

Table S2. Fit Parameters for Each Temperature-Dependent Isotherm to Redlich-Peterson Adsorption Model.

Temperature (°C)	A ($torr^{-1}$)	B ($torr^{-1}$)^g	g	K°	$\Delta G°_{ads}$
21	16.5 ± 1.8	16.7 ± 0.3	0.95 ± 0.01	9109.4	-22.6
38	7.3 ± 1.1	7.2 ± 1.2	0.97 ± 0.03	4484.6	-20.8
48	4.0 ± 0.5	3.7 ± 0.5	0.99 ± 0.03	2631.5	-19.5
58	2.6 ± 0.3	2.3 ± 0.3	0.99 ± 0.03	1635.8	-18.3
68	2.1 ± 0.2	1.6 ± 0.2	0.99 ± 0.04	1138.0	-17.4

Table S3. Fit Parameters for Each Temperature-Dependent Isotherm to Langmuir Adsorption Model.

Temperature (°C)	a	K($torr^{-1}$)	K°	$\Delta G°_{ads}$
21	1.0 ± 0.01	9.2 ± 0.1	6992	-21.9
38	1.0 ± 0.01	6.0 ± 0.6	4560	-20.9
48	1.1 ± 0.02	3.6 ± 0.3	2736	-19.6
58	1.2 ± 0.03	2.2 ± 0.2	1672	-18.4
68	1.2 ± 0.03	1.9 ± 0.2	1444	-18.0

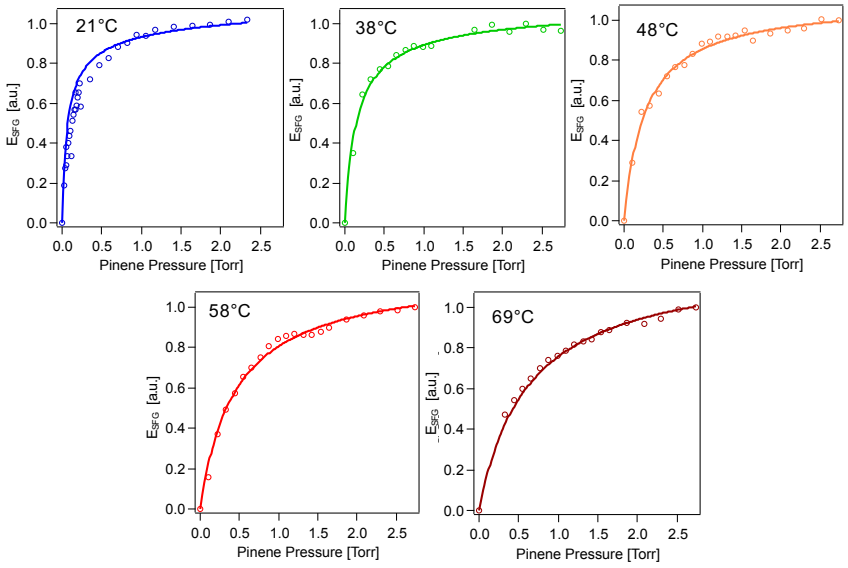

Figure S8. Adsorption isotherm fits to standard Redlich-Peterson adsorption model.

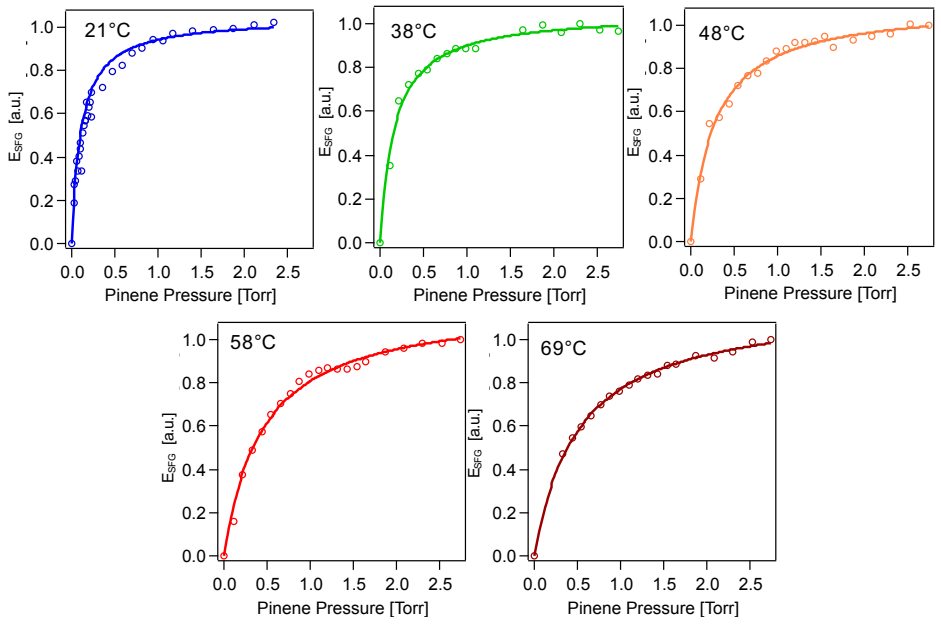

Figure S9. Adsorption isotherm fits to standard single-site Langmuir adsorption model.

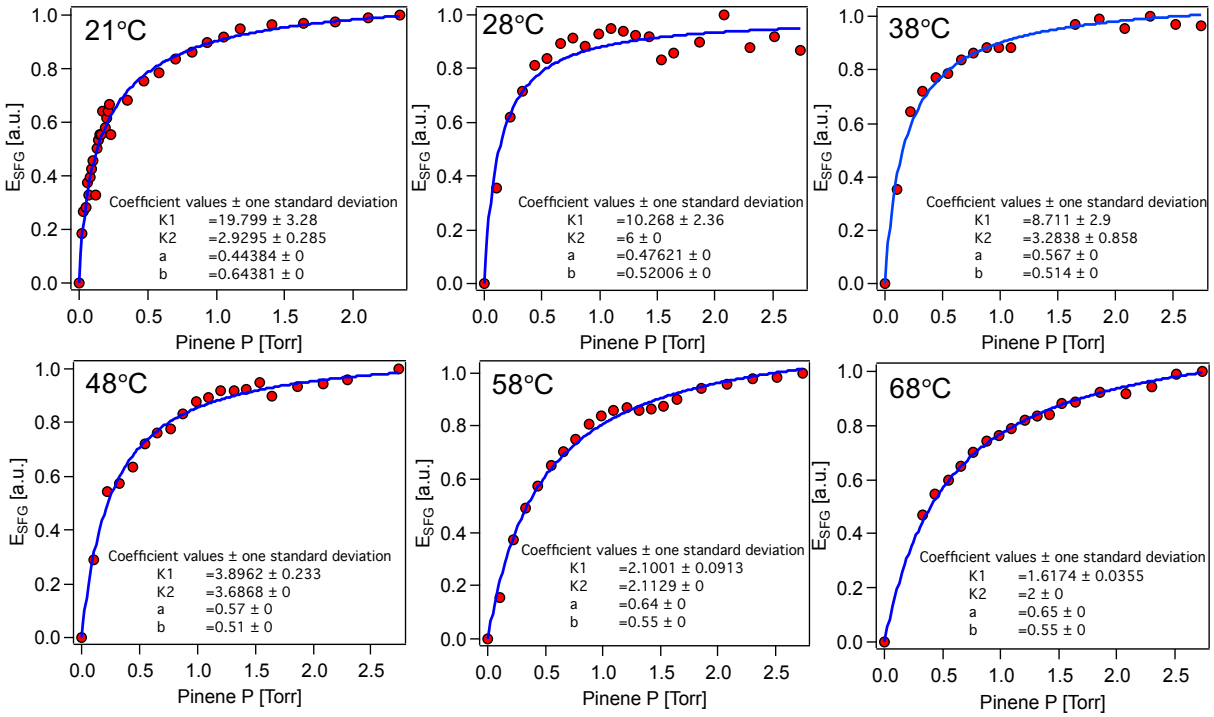

Figure S10. Adsorption isotherm data fit to dual-site Langmuir fits (blue trace) for each temperature. We assume K1 is the portion of α-pinene molecules that readily desorb.

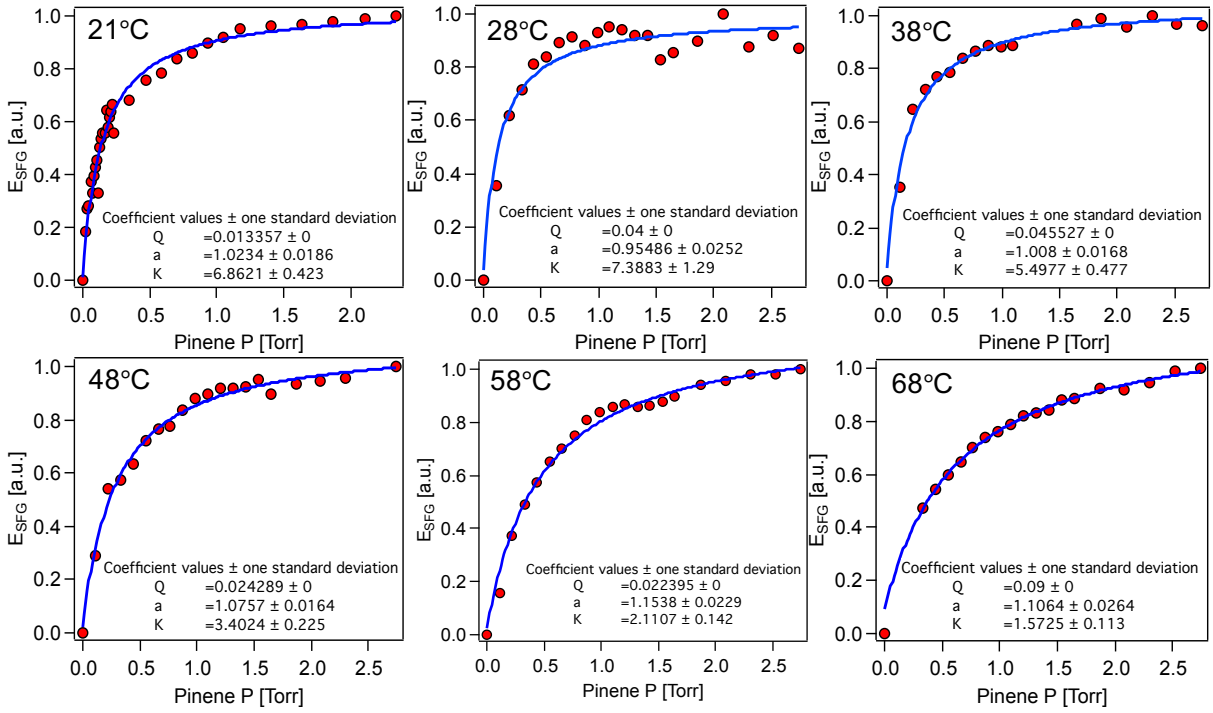

Figure S11. Adsorption isotherm fits to the dual-site model with irreversibility incorporated (blue trace).

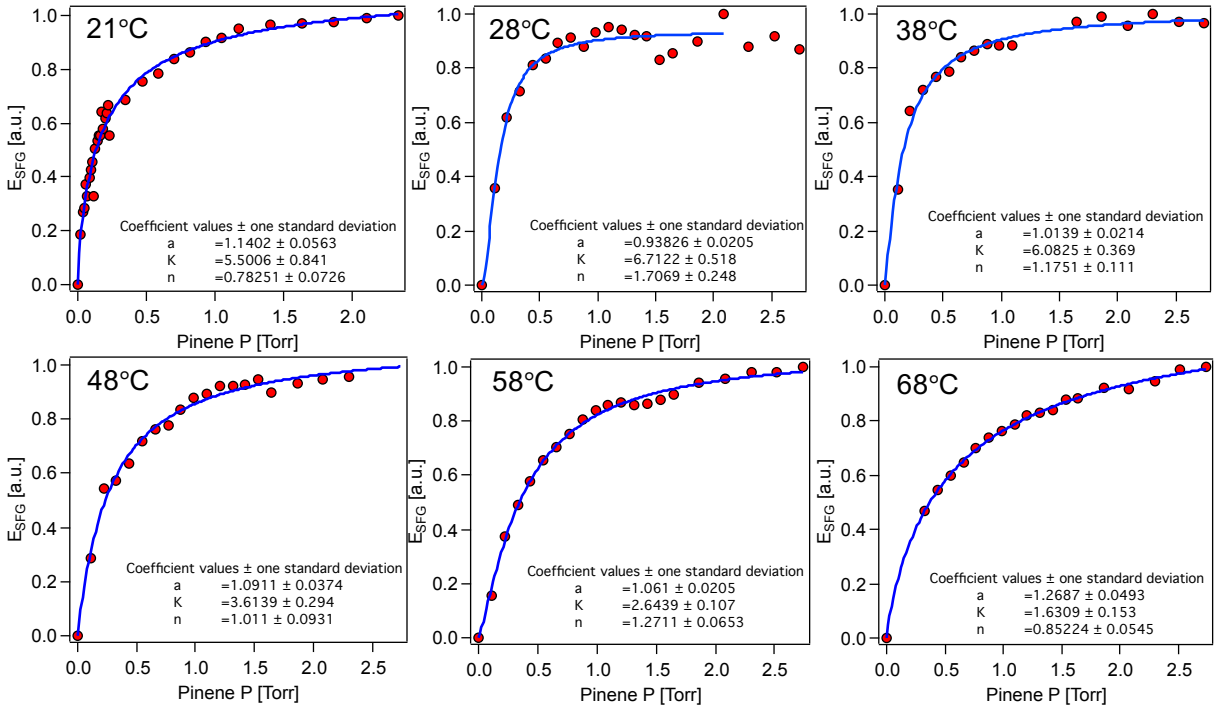

Figure S12. Adsorption isotherm fits to Langmuir-Freundlich adsorption model (blue trace).

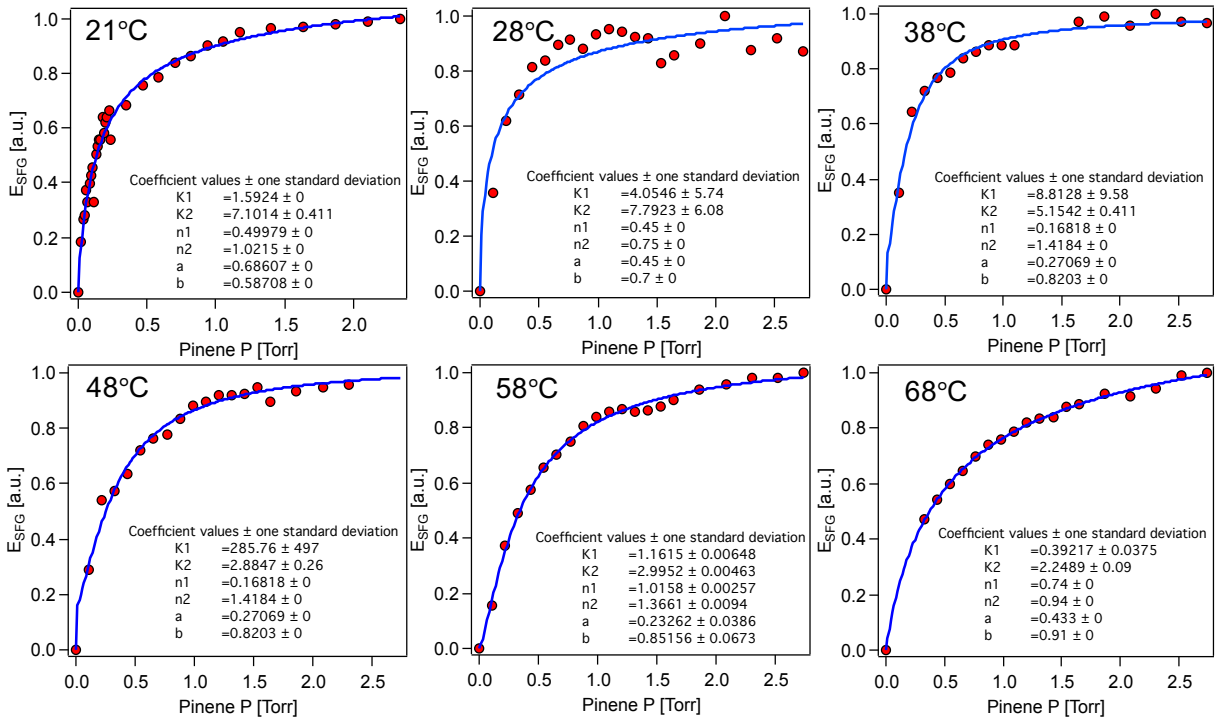

Figure S13. Adsorption isotherm fits to dual-site Langmuir-Freundlich adsorption model (blue trace).

Van't Hoff analysis is expressed by the following linear expression when plotting $\ln(K_{Ads})$ as a function of $(T)^{-1}$

$$y = a + bx \quad \text{(S2)},$$

wherein $y = K_{Ads}$; $x = \frac{1}{T}$; $a = \frac{\Delta S}{R}$; $b = \frac{-\Delta H}{R}$; and R=8.314 J $mol^{-1}K^{-1}$.

Table S4. Linear fit parameters from van't Hoff analysis: comparing Langmuir and Redlich-Peterson adsorption models.

Model	a	b
Langmuir	-3.4 ± 1	3600 ± 300
Redlich-Peterson	-6.8 ± 0.8	4700 ± 300

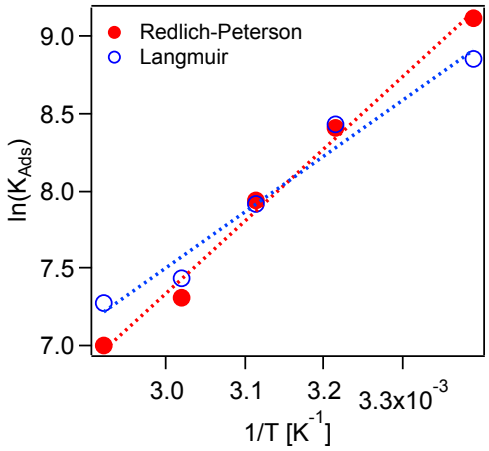

Figure S14. Redlich-Peterson (red filled circles) and Langmuir (blue unfilled circles) van't Hoff plots and their respective fits.

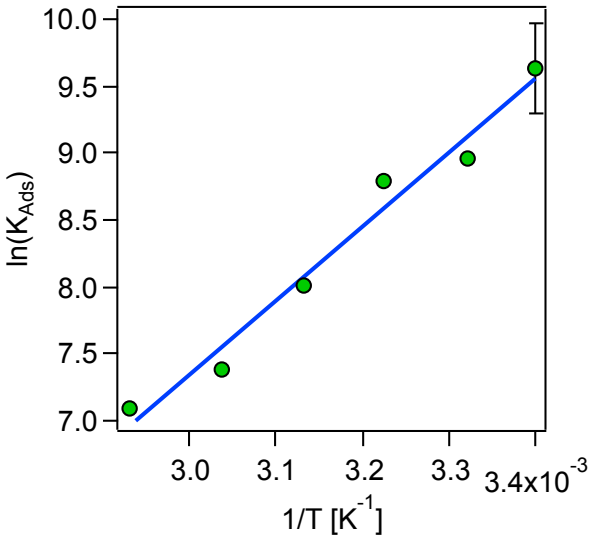

Figure S15. van't Hoff plot based on fits to dual-site Langmuir adsorption model, using one population from fit. The single error bar is associated with the largest error from isotherm fits at all temperatures.

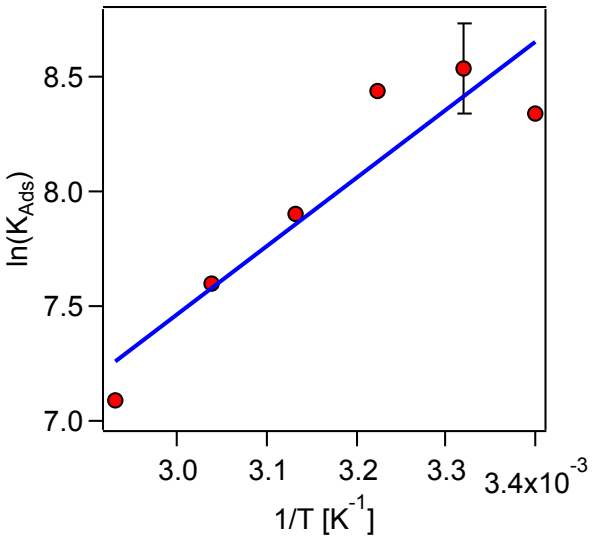

Figure S16. van't Hoff plot based on Langmuir-Freudlich fits. The single error bar is associated with the largest error from isotherm fits at all temperatures.

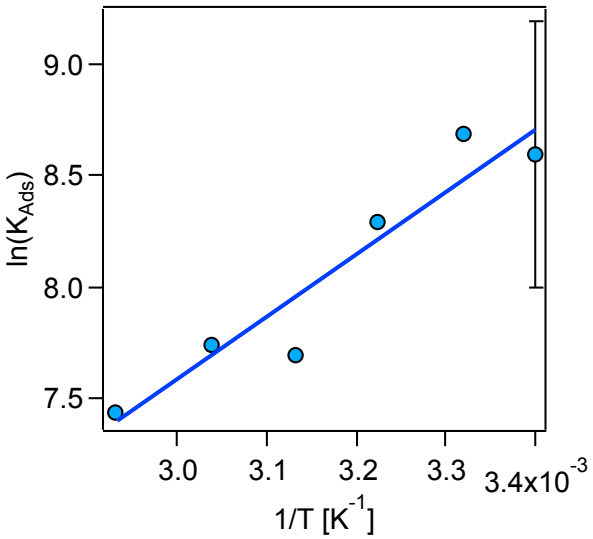

Figure S17. van't Hoff plot based on dual-site Langmuir-Freudlich fits. The single error bar is associated with the largest error from isotherm fits at all temperatures.

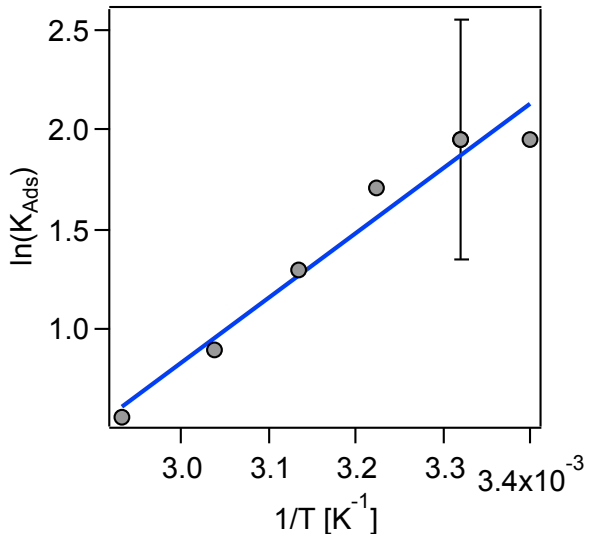

Figure S18. van't Hoff plot based on model incorporating irreversibility. The single error bar is associated with the largest error from isotherm fits at all temperatures.

S6. Reorientation Autocorrelation Function of Pinene-SiO_2 at Elevated Temperatures.

In our recent work, using MD simulations we computed two different reorientation times for α-pinene at 300 K. We carried out a similar analysis at 340 K to assess any potential differences in molecular orientation at elevated temperatures. The Z-component histogram is plotted in Fig. S over a 10 ns trajectory, and the molecular orientation distributions are similar for both 300 K and 340 K.

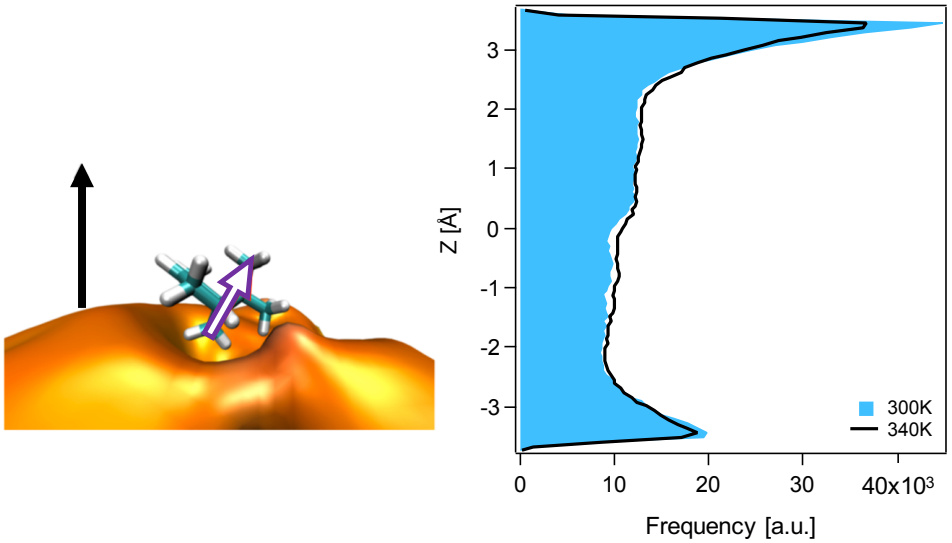

Figure S19. Comparison of the z-value histograms of α-pinene adsorbed to fused silica at 300 K (blue shading) and 340 K (black line).

Using this trajectory at 340 K, we computed a reorientation autocorrelation function for α-pinene molecules on silica, and fit the data to a double exponential function given by

$$y = a_0\left[a_1 \exp\left(-\frac{x}{\tau_1}\right) + (1-a_1)\exp\left(-\frac{x}{\tau_2}\right)\right] \quad \text{(S3)}.$$

From this fit we extract τ_1 of 1980 ps and τ_2 of 23 ps; whereas at 300 K these values were 2500 and 50 ps, respectively.

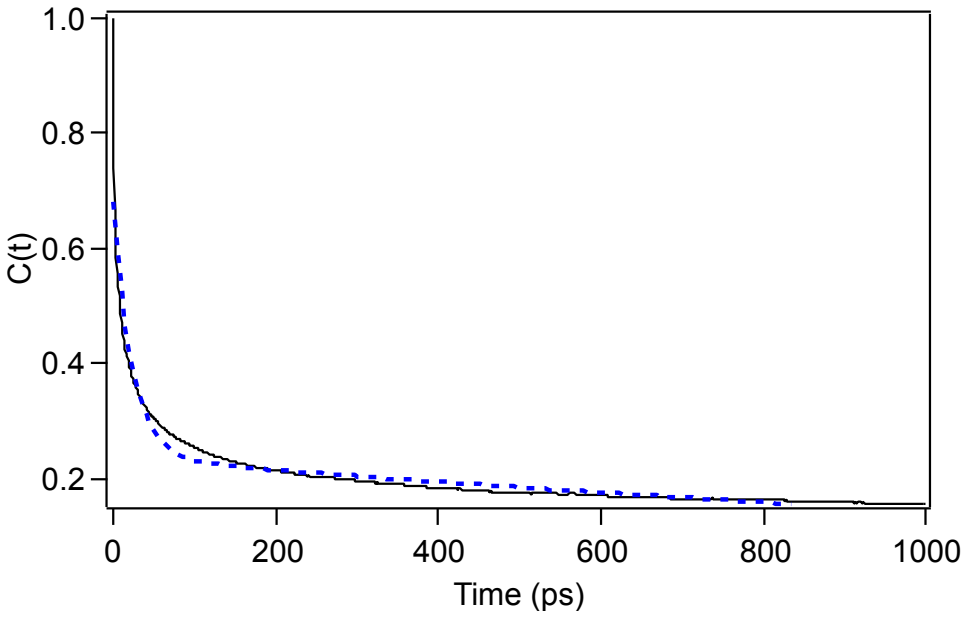

Figure S20. Reorientation autocorrelation function C(t) of α-pinene adsorbed to silica at 340K over 10 ns. Two reorientation times of 1980 ± 40 ps and 23 ± 0.5 ps is obtained from a double exponential fit (blue dotted line).

S7. Reversibility Studies.

We probed the reversibility of α-pinene to fused silica by alternating between α-pinene flow at various pressures and helium. We tried this for ~2.3, 0.1, and 0.02 Torr α-pinene. We were unable to obtain on-off traces for all pressures due to laser instability, therefore we took an average of 20 2-minute long spectra with pinene flow on and helium flow on to compare intensities and peak areas.

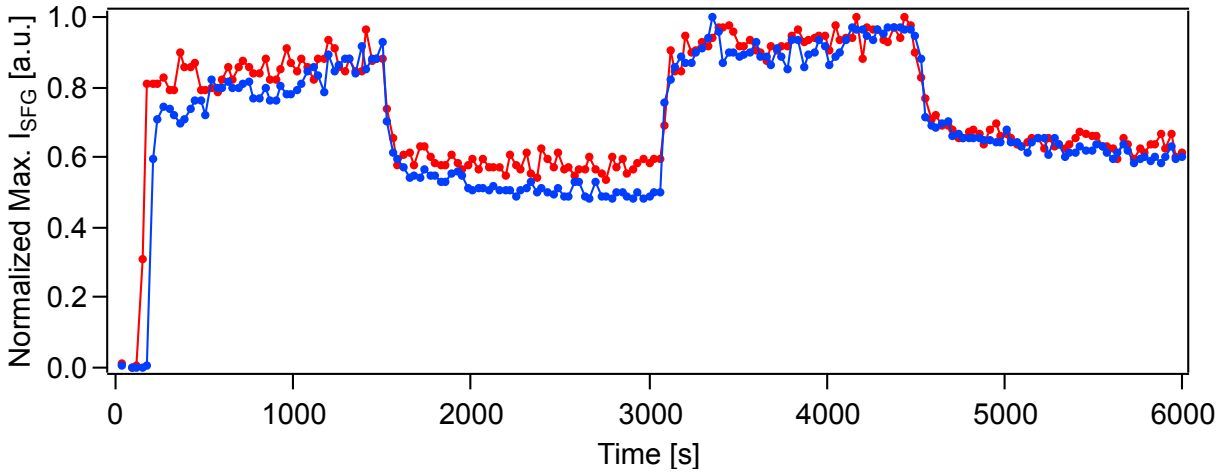

Figure S21. Two trials for on-off traces of 2.3 Torr α-pinene and helium. We plot maximum SFG signal intensity as a function of time.

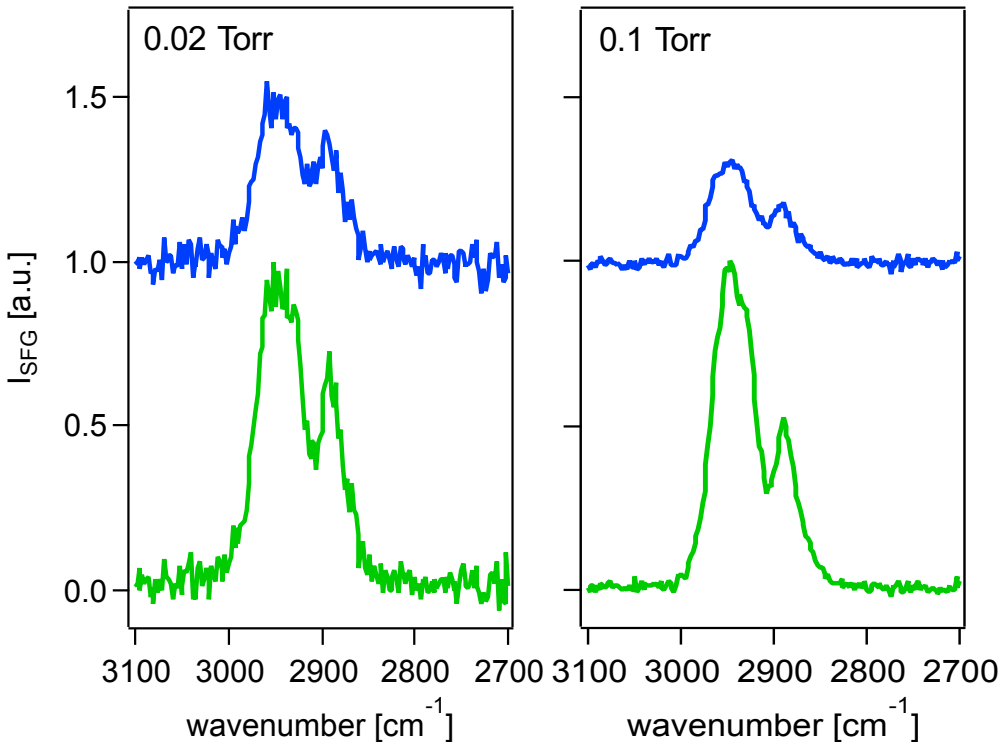

Figure S22. Average of 20 2-minute spectra with 0.02 and 0.1 Torr α-pinene flow on (green spectra) and helium flow on (blue spectra).

S8. Computational Details.

Table S5. Calculated adsorption enthalpies[a] at 300 K for individual α-pinene molecules from a 10 ns trajectory.

PINENE[b]	ΔH_{ads} (kJ/mol)	PINENE	ΔH_{ads} (kJ/mol)	PINENE	ΔH_{ads} (kJ/mol)
A59	-110.1	A31	-65.9	A20	-49.7
A99	-105.6	A96	-65.6	A12	-49.4
A23	-100.6	A72	-65.5	A127	-49.2
A71	-99.9	A89	-65.1	A42	-49.0
A40	-99.9	A28	-64.8	A81	-48.8
A69	-93.7	A115	-64.8	A78	-47.5
A58	-90.7	A10	-64.6	A121	-47.3
A49	-90.4	A88	-64.3	A64	-47.2
A66	-90.0	A33	-64.2	A50	-46.7
A113	-87.8	A62	-63.2	A46	-46.6
A80	-87.6	A119	-63.0	A26	-46.2
A22	-83.0	A68	-62.6	A95	-46.2
A67	-82.9	A41	-62.4	A7	-45.7
A130	-82.8	A85	-62.4	A116	-45.1
A44	-81.8	A19	-61.8	A4	-45.0
A90	-79.7	A29	-60.7	A84	-43.7
A24	-78.8	A53	-60.3	A32	-43.3
A92	-78.6	A15	-59.2	A112	-43.1
A73	-78.1	A94	-58.2	A27	-43.0
A93	-77.6	A43	-57.5	A13	-42.7
A6	-77.2	A5	-57.4	A101	-42.7
A86	-77.2	A110	-56.9	A98	-42.3
A97	-76.7	A114	-56.3	A51	-42.2
A38	-75.9	A129	-55.9	A16	-42.1
A30	-74.7	A111	-55.8	A45	-41.4
A83	-74.0	A63	-55.3	A57	-41.3
A105	-73.9	A128	-55.2	A65	-41.3
A47	-72.7	A60	-54.6	A100	-41.0
A11	-72.5	A9	-54.1	A25	-40.9
A39	-72.1	A18	-53.9	A102	-39.7
A61	-71.8	A21	-53.9	A74	-39.5
A106	-71.1	A8	-53.4	A91	-39.3
A104	-70.8	A70	-53.2	A122	-37.7
A1	-70.5	A118	-52.4	A123	-37.1
A17	-70.2	A56	-52.0	A126	-36.5
A87	-69.9	A82	-51.9	A125	-36.1
A75	-69.6	A2	-51.8	A77	-35.8
A124	-69.6	A117	-51.7	A52	-35.6

A36	-69.4	A54	-50.9	A37	-34.4
A3	-68.1	A103	-50.6	A14	-33.7
A34	-67.3	A108	-50.3	A35	-33.5
A120	-66.5	A55	-50.0	A107	-31.0
A109	-66.2	A76	-49.8	A79	-29.6
				A48	-26.4

[a] Enthalpies have been corrected by 12.2 kJ mol^{-1} according to comparison between CHARMM and ωB97XD/6-31G(d) calculations. [b] Numbering of different α-pinene molecules.

Table S6. Comparison of CHARMM versus ωB97XD/6-31G(d) interaction energies (in kJ mol^{-1}) for selected snapshots of α-pinene and silica based on a cluster model.

Snapshot	MM E(int)	QM E(int)	ΔE
1	-79.8	-65.0	-14.8
2	-73.1	-62.6	-10.6
3	-58.3	-46.7	-11.6
4	-59.7	-49.3	-10.5
5	-69.2	-52.8	-16.4
6	-65.0	-51.9	-13.1
7	-48.5	-42.3	-6.3
8	-73.3	-58.5	-14.7
9	-63.7	-52.6	-11.2
10	-65.8	-48.2	-17.6
11	-57.4	-46.5	-10.8
12	-58.0	-48.6	-9.4
13	-57.4	-49.4	-8.0
14	-73.0	-56.7	-16.3
		MAD	-12.2